The Journal of Chemical Physics

Accurate electron affinity of Ga and fine structures of its anions

Cite as: J. Chem. Phys. **152**, 114303 (2020); https://doi.org/10.1063/1.5144962
Submitted: 13 January 2020 . Accepted: 06 March 2020 . Published Online: 20 March 2020

Rulin Tang, Xiaoxi Fu, Yuzhu Lu, and Chuangang Ning

The Journal of Chemical Physics ARTICLE scitation.org/journal/jcp

Accurate electron affinity of Ga and fine structures of its anions

Cite as: J. Chem. Phys. 152, 114303 (2020); doi: 10.1063/1.5144962
Submitted: 13 January 2020 • Accepted: 6 March 2020 •
Published Online: 20 March 2020

Rulin Tang,[1] Xiaoxi Fu,[1] Yuzhu Lu,[1] and Chuangang Ning[1,2,a)]

AFFILIATIONS

[1] Department of Physics, State Key Laboratory of Low-Dimensional Quantum Physics, Tsinghua University, Beijing 100084, China
[2] Collaborative Innovation Center of Quantum Matter, Beijing 100084, China

[a)] **Author to whom correspondence should be addressed:** ningcg@tsinghua.edu.cn

ABSTRACT

We report the high-resolution photoelectron spectra of negative gallium anions obtained via the slow-electron velocity-map imaging method. The electron affinity of Ga is determined to be 2429.07(12) cm^{-1} or 0.301 166(14) eV. The fine structures of Ga are well resolved: 187.31(22) cm^{-1} or 23.223(27) meV for $^3P_1$ and 502.70(28) cm^{-1} or 62.327(35) meV for $^3P_2$ above the ground state $^3P_0$, respectively. The photoelectron angular distribution for photodetachment from $Ga^-(4s^24p^2\ ^3P_0)$ to $Ga(4s^25s\ ^2S_{1/2})$ is measured. An unexpected perpendicular distribution instead of an isotropic distribution is observed, which is due to a resonance near 3.3780 eV.

I. INTRODUCTION

Gallium is a technology-critical element for the modern semiconductor industry. Chemical compounds of gallium are widely used in microwave circuits, high-speed switching circuits, and infrared circuits.[1] In contrast to the extensive studies and widespread applications of gallium and its alloys,[2–5] our knowledge is rather limited regarding the atomic anion Ga^-. A negative ion is a distinct system from its neutral and positive counterparts as the extra electron is bound to the neutral core via the short-range force rather than the Coulomb binding force.[6] The electron affinity (EA), defined as the energy difference between the negative ion and the corresponding neutral atom (both in their ground states), is one of the most important parameters of an element and is also a preferable benchmark for the theoretical and computational models. The earliest EA value of Ga, 0.30(15) eV, was inferred by the semi-empirical extrapolation of a photodetachment threshold experiment.[7] Then, several theoretical results were reported, leaving EA values close to 0.3 eV.[8–15] In 2016, Wang *et al.* predicted the EA value to be 0.429 eV using the non-relativistic B-spline R-matrix method.[16] In 2019, Finney *et al.* predicted the EA value to be 0.302(22) eV using the relativistic coupled-cluster version of the Feller–Peterson–Dixon composite method.[17,18] The first experimental EA value of Ga was determined to be 0.4(2) eV by Cha *et al.*[19] Later, it was updated as 0.43(3) eV by Williams *et al.*[20] Recently, Gibson *et al.* reported an improved result of the EA value of Ga and the fine structures of Ga^- using the traditional laser photodetachment threshold (LPT) method.[21] They determined the electron affinity of Ga to be 301.20(11) meV and the fine structure splittings of Ga^- to be 23.31(19) meV for $J = 0–1$ and 62.4(5) meV for $J = 0–2$. They also reported high-level calculated results. The calculated electron affinity is 302(3) meV, and the fine structure splittings are 22(2) meV for $J = 0–1$ and 60(2) meV for $J = 0–2$.

In the present work, we report the photoelectron spectra of Ga^- using the slow-electron velocity-map imaging (SEVI) method, which has a very impressive energy resolution, typically a few cm^{-1} for low-energy electrons. The fine structures of Ga^- are well resolved. With the SEVI method, we have successfully measured EA values of many transitional elements with an accuracy ~1 cm^{-1}, such as Nb,[22] Hf,[23] Re,[24] La,[25] and Fe.[26] In the present work, we measured the EA values of three elements in the main group, i.e., Ga, I, and S. The EA values of I and S have been measured with a high accuracy via the laser photodetachment microscopy (LPM) method by Blondel and co-workers.[27–30] We present the results of I and S here for the comparison of the two methods.

II. METHODS

The experiment is conducted using our newly built photoelectron-imaging spectrometer featured with the combination of the SEVI technique and the cryogenically controlled ion trap.[31,32]

The detailed description of the spectrometer has been reported previously.[33] Ga anions are produced via the pulsed Nd:YAG laser ablation of a gallium metal ball. Generated anions lose their kinetic energy through collisions with a burst of buffer gas (typically 20%H_2 + 80%He) in an octupole radio frequency (rf) ion trap, which is mounted on the second stage of a liquid helium refrigerator, with a controllable temperature in the range of 5–300 K. After being confined for 45 ms, the stored anions are extracted and analyzed by using a Wiley–McLaren type time-of-flight (TOF) mass spectrometer.[34] Ga has two stable isotopes, ^{69}Ga (60.11%) and ^{71}Ga (39.89%). The anions with m = 69 are chosen as our research target for its higher natural abundance and are then perpendicularly crossed by the detachment laser beam with an adjustable wavelength in the interaction zone of the velocity-map imaging (VMI) system.[35] The outgoing electrons with the same velocity form an expanding spherical shell and are projected onto a phosphor screen intensified by two micro-channel plates. The electron hitting positions are recorded in an event-count mode via a CCD camera and accumulated typically for 50 000 laser shots. The apparatus runs at a 20-Hz repetition rate. Since the distribution of the outgoing photoelectrons has a cylindrical symmetry, the 3D photoelectron spherical shell can be reconstructed from the projected 2D image by performing an inverse Abel transform[36] or by inverting the image without Abel inversion, as done here with the help of the maximum entropy velocity Legendre reconstruction (MEVELER) method.[37] The advantage of the MEVELER method is that there is no center-line-noise problem. The binding energy (BE) can be deduced by BE = $h\nu - \alpha r^2$, where hν is the photon energy, r is the radius of the spherical shell, and the α is a calibration coefficient. The photoelectron angular distribution (PAD) can also be extracted from the reconstruction. For one-photon detachment with a linearly polarized laser, the PAD is given by the expression[38]

$$I(\theta) = \frac{\sigma}{4\pi}[1 + \beta P_2(\cos\theta)]. \quad (1)$$

Here, θ is the angle of the outgoing electron relative to the laser polarization, and P_2 is the second-order Legendre polynomial. σ is the total photodetachment cross section. β is defined as the asymmetry parameter with a value lying between 2 and −1. The β value reflects the different partial waves of the emitted electron and the energy-dependent interference between them.

Recently, we also measured the EA value of Pb, an element in the main group. For the main-group elements, it is an s-wave photodetachment near the photodetachment threshold, which is in contrast to the p-wave photodetachment for transitional elements. EA values of most main-group elements were measured using the LPM method by Blondel and co-workers.[39–41] The LPM method, based on the interference effect, usually requires the photoelectron energy to be lower than 1 cm^{-1}. According to the Wigner threshold law,[42] the p-wave photodetachment cross section near the threshold is very low. So far, there is no LPM experiment reported for a p-wave photodetachment. The advantage of SEVI is that it can achieve a typical energy resolution of a few cm^{-1} for the photoelectron kinetic energy ~100 cm^{-1}. In 2016, we measured the binding

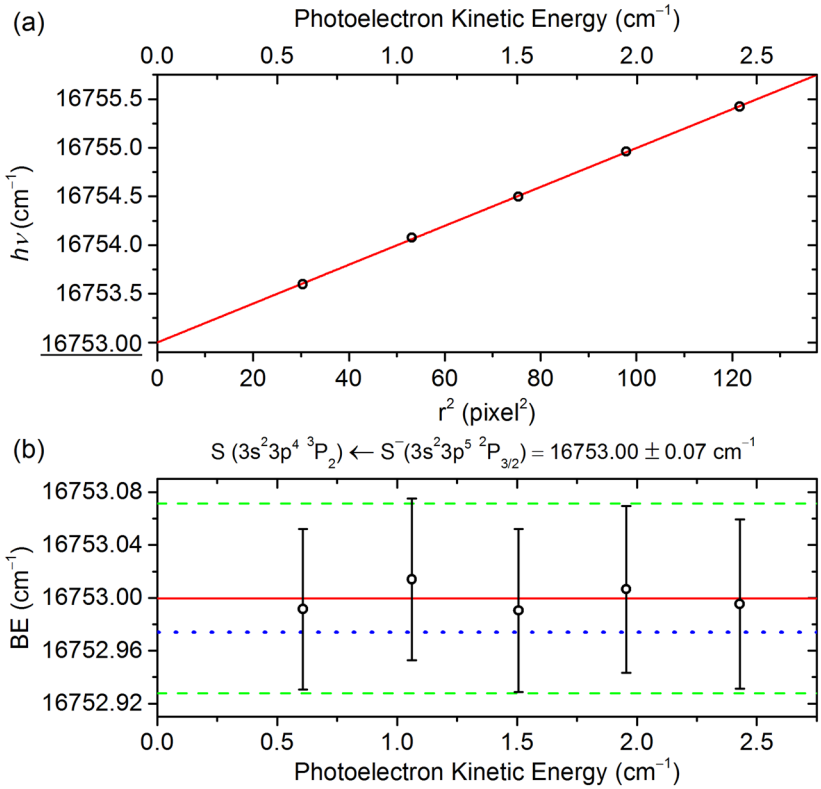

FIG. 1. (a) The photon energy $h\nu$ vs the squared radius r^2 of the photoelectrons spherical shell for the transition S^- ($3s^23p^5\ ^2P_{3/2}$) → S ($3s^23p^4\ ^3P_2$). The solid line is the linear least squares fitting. The intercept 16 753.00(7) cm^{-1} is the binding energy of this photodetachment channel. (b) The binding energy as a function of the kinetic energy of photoelectrons. The dashed lines indicate the uncertainty of ±0.07 cm^{-1}. The red solid line represents the binding energy obtained via our SEVI method. The LPM result is also plotted as a blue dotted line for comparison.

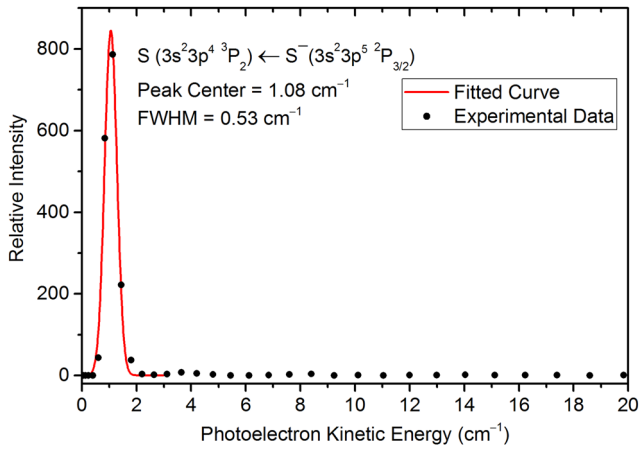

FIG. 2. Photoelectron spectrum of S^- obtained at $h\nu$ = 16 754.08 cm^{-1}. The averaged kinetic energy of photoelectrons is 1.08 cm^{-1}. The peak corresponds to the transition S^- ($3s^2 3p^5$ $^2P_{3/2}$) → S ($3s^2 3p^4$ $^3P_2$). The FWHM is 0.53 cm^{-1}.

energies of photodetachment channel $^4S_{3/2} \rightarrow {}^3P_2$ of ^{206}Pb, ^{207}Pb, and ^{208}Pb separately using the SEVI method and obtained an EA value of 0.356 743(16) eV for the isotope m = 208.[43] In 2018, Blondel and co-workers measured an isotope-averaged binding energy of the photodetachment channel $^4S_{3/2} \rightarrow {}^3P_{1,2}$.[44] They obtained 0.356 721(2) eV by assuming that the isotope shift of the electron affinity would remain smaller than the total uncertainty. It can be seen that there is a slight discrepancy. The reason behind the discrepancy is not clear since two different photodetachment channels were used for different isotopes. Therefore, it is worthy to directly compare SEVI and LPM methods for other main-group elements. In 2015, we measured the EA value of iodine (I) using our first-generation apparatus and obtained EA(I) = 24 672.94(10) cm^{-1}. Our result is consistent with the EA value 24 672.874(29) cm^{-1} obtained by the Blondel group using the LPM method.[28] Recently, we determined the EA value of S to be 16 753.00(7) cm^{-1} using our second-generation apparatus (see Fig. 1), which has a higher energy resolution than our first apparatus. Our result is in an excellent agreement with the LPM result [16 752.9753(41) cm^{-1}].[30] The slight difference (0.025 cm^{-1}) primarily comes from the accuracy of our wavelength meter (0.02 cm^{-1}) and the linewidth of the dye laser (0.06 cm^{-1}), which are also the dominant sources of the uncertainty. Figure 2 shows a typical photoelectron energy spectrum obtained with our second-generation machine at an imaging voltage −150 V. The energy resolution [the full width at half maximum (FWHM)] is 0.53 cm^{-1} for the peak with the electron kinetic energy E_k = 1.08 cm^{-1}. It is comparable with 1.2 cm^{-1} for E_k = 5.2 cm^{-1} reported by the Wang group[35] and 1.1 cm^{-1} for E_k = 1.8 cm^{-1} by the Neumark group.[45]

III. RESULTS AND DISCUSSION

Figure 3 presents the spectrum obtained at wavelengths λ = 2600 nm and 365 nm using an optical-parametric-oscillator (OPO) laser. The linewidth of our OPO system is about 5 cm^{-1}. In the present work, the temperature of the ion trap is kept at 300 K and the trap time is 45 ms. Nine sharp peaks relevant to different transitions from $4s^2 4p^2$ ^3P fine structures are well resolved and labeled *a*–*i*. The diagram of the transitions is illustrated in Fig. 4. To accurately determine the EA value, we further measured the spectrum using our narrow-linewidth dye laser. Peaks *c*, *f*, and *i* correspond to the transitions from the ground state $4s^2 4p^2$ $^3P_0$. Since the binding energies of peaks *c* and *f* are out of the tuning range of our dye laser, peak *i*, related to the transition $^3P_0 \rightarrow {}^2S_{1/2}$, is selected as the target channel for the present EA measurement. The second harmonic generation (SHG, linewidth 0.09 cm^{-1}) of the dye laser is used to photodetach Ga^- anions near the threshold. The dye laser (Spectra-physics) is pumped by using a 532-nm Nd:YAG laser (Quanta-Ray Pro 190),

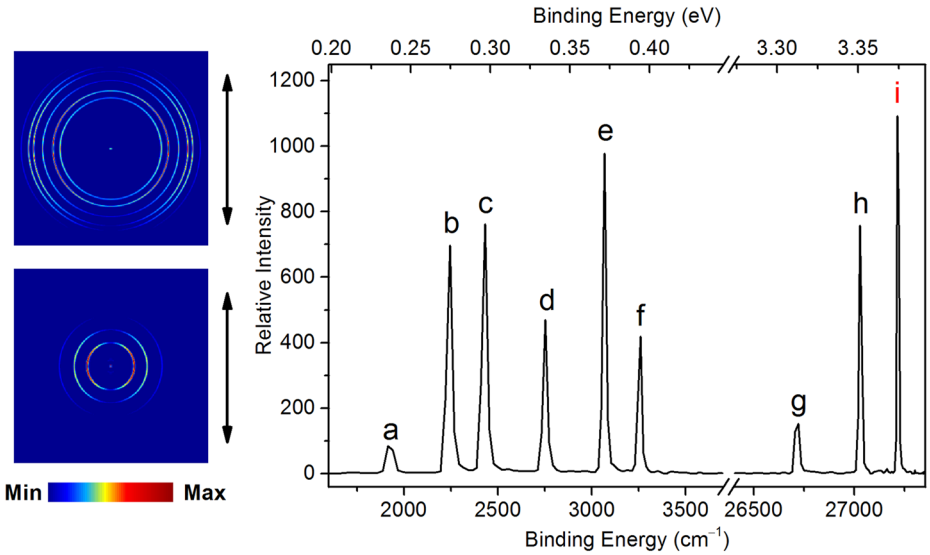

FIG. 3. Photoelectron images and spectra for Ga^-. Peaks *a*–*f* and peaks *g*–*i* were observed at 2600 nm and 365 nm, respectively. They were pieced together for a better view with an arbitrary intensity scale. The measured intensity ratio of peak *i* to the summed intensity of peaks *a*–*f* can be found in Fig. 6. The double arrow indicates the polarization of the photodetachment laser. Peak *i* is related to the transition Ga^-($4s^2 4p^2$ $^3P_0$) → Ga($4s^2 5s$ $^2S_{1/2}$), which is used to measure the electron affinity of Ga in the present work.

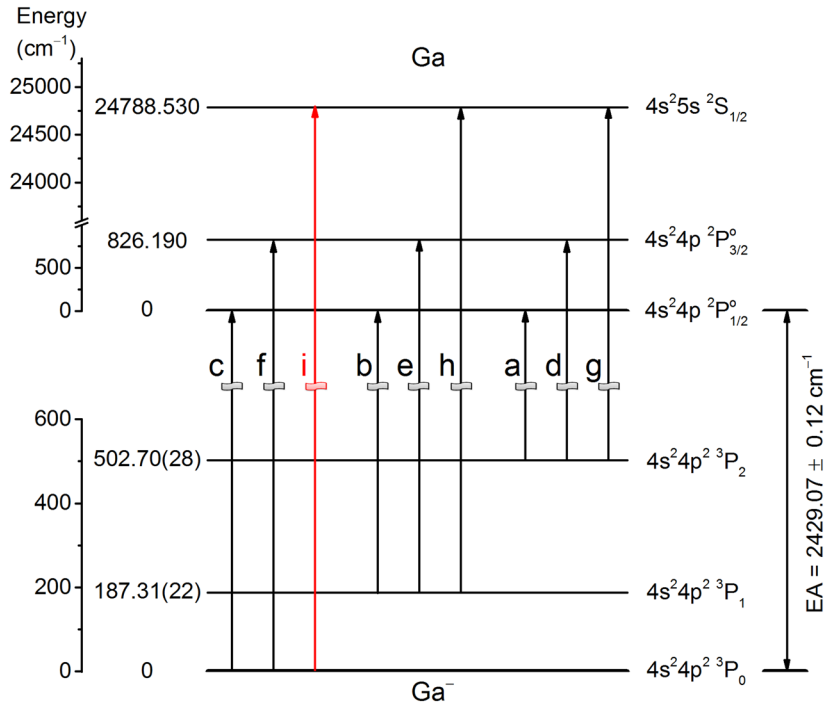

FIG. 4. Energy levels of Ga^- and Ga related to the present measurement. The ground state of Ga is $4s^24p\ ^2P_{1/2}$. The ground state of Ga^- is $4s^24p^2\ ^3P_0$. The labels of each transition are the indices of the observed peaks in Fig. 3. The transition *i* is used for the electron affinity measurement.

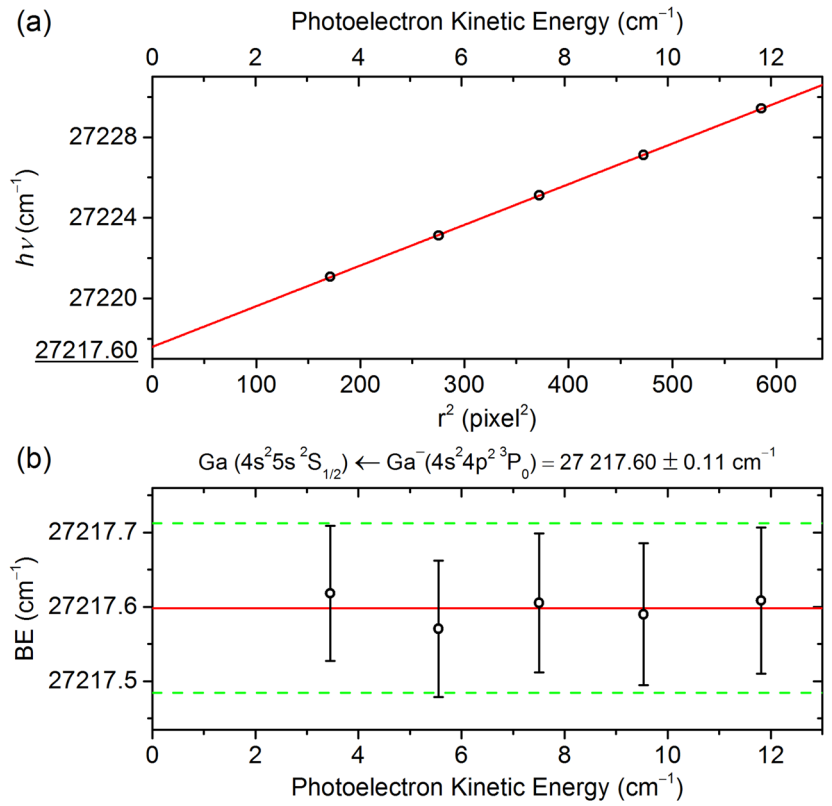

FIG. 5. (a) The photon energy $h\nu$ vs the squared radius r^2 of the photoelectron spherical shell for transition *i*. The solid line is the linear least squares fitting. The intercept 27 217.60(11) cm^{-1} is the binding energy of photodetachment channel *i*. (b) The binding energy of transition *i* as a function of the kinetic energy of photoelectrons. The dashed lines indicate the uncertainty of ±0.11 cm^{-1}.

TABLE I. Summary of the fine structures of Ga^- and the electron affinity results of Ga.

Fine structures of Ga^- (meV)			
Levels	Gibson *et al.*[21] (calculated)	Gibson *et al.*[21] (measured)	This work (measured)
$^3P_1 \leftarrow {}^3P_0$	22(2)	23.31(19)	23.223(27)
$^3P_2 \leftarrow {}^3P_0$	60(2)	62.4(5)	62.327(35)

Electron affinity of Ga	
Value	References[a]
0.429 eV	Wang *et al.*[16] (calculated)
0.302(22) eV	Finney and Peterson[17,18] (calculated)
0.302(3) eV	Gibson *et al.*[21] (calculated)
0.4(2) eV	Cha *et al.*[19] (measured)
0.43(3) eV	Williams *et al.*[20] (measured)
0.301 20(11) eV	Gibson *et al.*[21] (measured)
0.301 166(14) eV or 2429.07(12) cm^{-1}	This work (measured)

[a]Only three latest calculated results listed.

and the second harmonic is generated by the built-in $LiNbO_3$ crystal. The wavelength is continuously monitored by using a wavelength meter (HighFinesse WS6-600) with an accuracy of 0.02 cm^{-1}.

To accurately determine the BE of peak *i*, the photon energy $h\nu$ was varied from 27 221 cm^{-1} to 27 229 cm^{-1} with a step of 2 cm^{-1}, slightly above the threshold. Since $h\nu = BE + \alpha r^2$, the experimental data are plotted as $h\nu$ vs r^2 in Fig. 5. The intercept of the fitted line gives the BE value 27 217.60(11) cm^{-1}. The final state of transition *i* is 24 788.530(7) cm^{-1} above the ground state.[46,47] As a result, the EA value of Ga is determined to be 2429.07(12) cm^{-1} or 0.301 166(14) eV. Note that 1 eV = 8065.543 937... cm^{-1}, as recommended by 2018 CODATA.[48]

Note that transitions *g*, *h*, and *i* are from different fine-structure states to the same final state $^2S_{1/2}$. Therefore, the fine-structure splittings can be obtained from the differences among them. Two more spectra are acquired at $h\nu$ = 26 724 cm^{-1} and 27 039 cm^{-1} using the SHG output of our dye laser system, which are slightly above the threshold of peaks *g* and *h*, respectively. Then, the BEs of the two transitions are deduced via $BE = h\nu - \alpha r^2$. Finally, the energy levels of the two fine-structure excited states $^3P_1$ and $^3P_2$ are determined as 187.31(22) cm^{-1} or 23.223(27) meV and 502.70(28) cm^{-1} or 62.327(35) meV above the ground state $^3P_0$, respectively. The EA value and the fine structure levels reported in this work are summarized and compared with previous results in Table I. Our results are in excellent agreement with Gibson's values, but the accuracy is improved by a factor of 10. The related transitions, energy levels, and asymmetry parameters for peaks *a*–*i* are summarized in Table II. It can be seen that all transitions have negative β values ranging

TABLE II. Measured binding energies, assigned binding energies, and asymmetry parameters β of the transitions observed in the present work.

Peak	Levels ($Ga^- \rightarrow Ga$)	Measured binding energy (cm^{-1})	Assigned binding energy (cm^{-1})[a]	Asymmetry parameter β[b]
a	$4s^24p^2\ {}^3P_2 \rightarrow 4s^24p\ {}^2P_{1/2}$	1926.2(60)	1926.37(25)	−0.93
b	$4s^24p^2\ {}^3P_1 \rightarrow 4s^24p\ {}^2P_{1/2}$	2241.9(57)	2241.76(18)	−0.97
c	$4s^24p^2\ {}^3P_0 \rightarrow 4s^24p\ {}^2P_{1/2}$	2429.3(56)	2429.07(11)	−0.95
d	$4s^24p^2\ {}^3P_2 \rightarrow 4s^24p\ {}^2P_{3/2}$	2752.3(53)	2752.56(25)	−0.82
e	$4s^24p^2\ {}^3P_1 \rightarrow 4s^24p\ {}^2P_{3/2}$	3067.7(52)	3067.95(18)	−0.61
f	$4s^24p^2\ {}^3P_0 \rightarrow 4s^24p\ {}^2P_{3/2}$	3255.5(51)	3255.26(11)	−0.49
g	$4s^24p^2\ {}^3P_2 \rightarrow 4s^25s\ {}^2S_{1/2}$	26 714.90(25)	26 714.90(25)	−0.87
h	$4s^24p^2\ {}^3P_1 \rightarrow 4s^25s\ {}^2S_{1/2}$	27 030.29(18)	27 030.29(18)	−0.90
i	$4s^24p^2\ {}^3P_0 \rightarrow 4s^25s\ {}^2S_{1/2}$	27 217.60(11)	27 217.60(11)	−0.93

[a]Deduced value according to the energy levels of neutral atoms and the binding energies of transitions *g*, *h*, and *i*.
[b]β values of peaks *a*–*f* are obtained at the wavelength λ = 2600 nm and peaks *g*–*i* at λ = 365 nm.

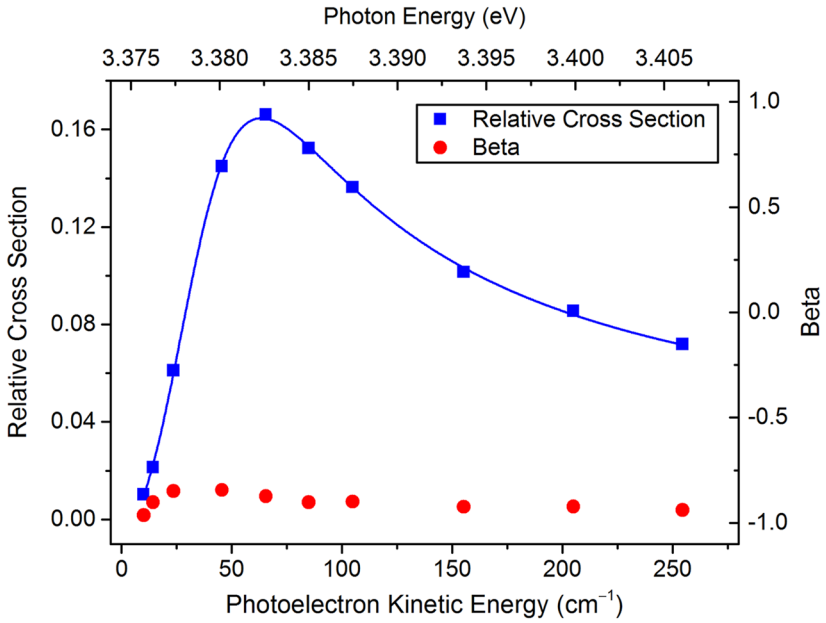

FIG. 6. The relative cross sections and the β values of the transition *i* as a function of the kinetic energy of photoelectrons. The blue curve comes from the fitting to Eq. (2).

from −0.5 to −1. The trend of β values of peaks *a*–*f* is consistent with the behavior of a *p*-electron photodetachment that the β value decreases from 0 to −1 and then returns to 0 as E_k increases due to the interference of the *s*-wave and the *d*-wave.[38,49,50]

During the experiment, we observed a resonance near $h\nu = 3.3780$ eV as we scanned the photon energy. Since the intensity of the Ga^- ion beam has a pulse-to-pulse fluctuation, the relative cross section is measured as the ratio of the intensity of peak *i* to the summed intensity of peaks *a*–*f*. Compared with the large kinetic energies (>24 000 cm^{-1}) of peaks *a*–*f*, the scanning range ~250 cm^{-1} is relatively small. Therefore, it is reasonable to assume that their photodetachment cross sections are constant. The relative cross sections and the β values of the transition *i* are plotted in Fig. 6. Similar resonance curves have been observed previously in some other anion systems, such as He^-[51] and Os^-.[52] They were proven to be *p*-wave shape resonances, and the cross section could be described using the following equation:

$$\sigma = \sigma_0 + c(\varepsilon - \varepsilon_0)^{3/2}/[(\varepsilon - \varepsilon_r)^2 + (\Gamma/2)^2], \quad (2)$$

where σ_0 is the background, *c* is a constant, ε_0 is the threshold energy, ε_r is the resonance position, and Γ is the full width at half maximum (FWHM) parameter of the resonance. As can be seen in Fig. 6, the equation fits our observed data very well, which suggests that it is a shape resonance as well. The fitting gives ε_r = 27 245 cm^{-1} (3.3780 eV) and Γ = 83 cm^{-1}, so the resonance is 28 cm^{-1} above the threshold. Compared to the Γ values of the shape resonances in He^- [57.75(56) cm^{-1}] and Os^- [3.66(3) cm^{-1}], the Γ mentioned here is slightly larger, indicating a shorter lifetime of the metastable excited state.

We notice that the β value of peak *i* in the scanning region is almost a constant, close to −1 (see Fig. 6). Usually, the photodetachment from a *p* orbital near its threshold usually has an isotropic distribution ($\beta = 0$). The unexpected β values might be due to that the transition $4s^24p^2\ ^3P_0 \rightarrow 4s^25s\ ^2S_{1/2}$ is a two-electron process (one 4p electron is detached with another 4p electron excited to 5s) and it is an indirect photodetachment via a resonance. Additionally, since the parities of the initial state $4s^24p^2\ ^3P_0$ and the final state $4s^25s\ ^2S_{1/2}$ are both even, the final photoelectron cannot be an *s*-wave. Therefore, we cannot observe an isotropic photoelectron angular distribution. Wang *et al.* predicted a strong resonance at 3.543 eV due to a transition from the ground state of Ga^- $4s^24p^2\ ^3P$ to the excited continuum states $4s^25s5p\ ^3P°$.[16] However, the β value of the transition via $4s^25s5p\ ^3P°$ resonance is predicted to rapidly vary from −0.4 to 0.4 and then to −0.4 as the photon energy crosses the resonance from the lower side, rather than an almost constant value ($\beta \sim -1$) as observed in our experiment. Besides peak *i*, all β values we measured are far different from Wang's prediction. For example, peaks *a*–*f* at $h\nu$ = 2600 nm (0.48 eV) have beta values less than −0.49, rather than a value around 0 as predicted by Wang's calculation. In their calculations, a cut-off parameter is chosen to match the best available electron affinity at the time of that publication [0.43(3) eV], which is far away from our measurement [0.301 166(14) eV].

IV. CONCLUSIONS

In conclusion, we obtained the high-resolution photoelectron energy spectra of Ga^- using the SEVI method. The electron affinity of Ga was measured to be 2429.07(12) cm^{-1} or 0.301 166(14) eV. The fine structures of Ga^- were well resolved, and their energy levels were determined. In addition, a resonance near 3.3780 eV was observed.

ACKNOWLEDGMENTS

The authors gratefully acknowledge the discussions with Professor Bo Gao and Professor Chongyang Chen and Dr. Ran Si.

This work was supported by the National Natural Science Foundation of China (NSFC) (Grant Nos. 91736102 and 11974199) and the National Key R&D program of China (Grant No. 2018YFA0306504).

REFERENCES

[1] R. R. Moskalyk, Miner. Eng. **16**, 921 (2003).
[2] S. J. Adelman, C. R. Proffitt, G. M. Wahlgren, D. S. Leckrone, and L. Dolk, Astrophys. J., Suppl. Ser. **155**, 179 (2004).
[3] M. Leszczynski, H. Teisseyre, T. Suski, I. Grzegory, M. Bockowski, J. Jun, S. Porowski, K. Pakula, J. M. Baranowski, C. T. Foxon, and T. S. Cheng, Appl. Phys. Lett. **69**, 73 (1996).
[4] A. Polian, M. Grimsditch, and I. Grzegory, J. Appl. Phys. **79**, 3343 (1996).
[5] J. Goldberger, R. R. He, Y. F. Zhang, S. W. Lee, H. Q. Yan, H. J. Choi, and P. D. Yang, Nature **422**, 599 (2003).
[6] T. Andersen, Phys. Rep. **394**, 157 (2004).
[7] H. Hotop and W. C. Lineberger, J. Phys. Chem. Ref. Data **14**, 731 (1985).
[8] F. Arnau, F. Mota, and J. J. Novoa, Chem. Phys. **166**, 77 (1992).
[9] W. P. Wijesundera, Phys. Rev. A **55**, 1785 (1997).
[10] E. Eliav, Y. Ishikawa, P. Pyykkö, and U. Kaldor, Phys. Rev. A **56**, 4532 (1997).
[11] D. Sundholm, M. Tokman, P. Pyykkö, E. Eliav, and U. Kaldor, J. Phys. B: At., Mol. Opt. Phys. **32**, 5853 (1999).
[12] D. Figgen, A. Wedig, H. Stoll, M. Dolg, E. Eliav, and U. Kaldor, J. Chem. Phys. **128**, 024106 (2008).
[13] C. Guo-Xin and P. P. Ong, J. Phys. B: At., Mol. Opt. Phys. **32**, 5351 (1999).
[14] J. Li, Z. Zhao, M. Andersson, X. Zhang, and C. Chen, J. Phys. B: At., Mol. Opt. Phys. **45**, 165004 (2012).
[15] Z. Felfli, A. Z. Msezane, and D. Sokolovski, J. Phys. B: At., Mol. Opt. Phys. **45**, 189501 (2012).
[16] K. Wang, O. Zatsarinny, and K. Bartschat, Phys. Rev. A **94**, 023402 (2016).
[17] B. A. Finney and K. A. Peterson, J. Chem. Phys. **151**, 024303 (2019).
[18] B. A. Finney and K. A. Peterson, J. Chem. Phys. **151**, 159901 (2019).
[19] C.-Y. Cha, G. Ganteför, and W. Eberhardt, J. Chem. Phys. **100**, 995 (1994).
[20] W. W. Williams, D. L. Carpenter, A. M. Covington, M. C. Koepnick, D. Calabrese, and J. S. Thompson, J. Phys. B: At., Mol. Opt. Phys. **31**, L341 (1999).
[21] N. D. Gibson, C. W. Walter, C. Crocker, J. Wang, W. Nakayama, J. N. Yukich, E. Eliav, and U. Kaldor, Phys. Rev. A **100**, 052512 (2019).
[22] Z. H. Luo, X. L. Chen, J. M. Li, and C. G. Ning, Phys. Rev. A **93**, 020501 (2016).
[23] R. L. Tang, X. L. Chen, X. X. Fu, H. Wang, and C. G. Ning, Phys. Rev. A **98**, 020501(R) (2018).
[24] X. L. Chen and C. G. Ning, J. Phys. Chem. Lett. **8**, 2735 (2017).
[25] Y. Lu, R. L. Tang, X. X. Fu, and C. G. Ning, Phys. Rev. A **99**, 062507 (2019).
[26] X. L. Chen, Z. H. Luo, J. M. Li, and C. G. Ning, Sci. Rep. **6**, 24996 (2016).
[27] C. Blondel, W. Chaibi, C. Delsart, C. Drag, F. Goldfarb, and S. Kröger, Eur. Phys. J. D **33**, 335 (2005).
[28] R. J. Peláez, C. Blondel, C. Delsart, and C. Drag, J. Phys. B: At., Mol. Opt. Phys. **42**, 125001 (2009).
[29] W. Chaibi, R. J. Peláez, C. Blondel, C. Drag, and C. Delsart, Eur. Phys. J. D **58**, 29 (2010).
[30] T. Carette, C. Drag, O. Scharf, C. Blondel, C. Delsart, C. Froese Fischer, and M. Godefroid, Phys. Rev. A **81**, 042522 (2010).
[31] C. Hock, J. B. Kim, M. L. Weichman, T. I. Yacovitch, and D. M. Neumark, J. Chem. Phys. **137**, 244201 (2012).
[32] X. B. Wang and L. S. Wang, Rev. Sci. Instrum. **79**, 073108 (2008).
[33] R. L. Tang, X. X. Fu, and C. G. Ning, J. Chem. Phys. **149**, 134304 (2018).
[34] W. C. Wiley and I. H. McLaren, Rev. Sci. Instrum. **26**, 1150 (1955).
[35] I. León, Z. Yang, H.-T. Liu, and L.-S. Wang, Rev. Sci. Instrum. **85**, 083106 (2014).
[36] V. Dribinski, A. Ossadtchi, V. A. Mandelshtam, and H. Reisler, Rev. Sci. Instrum. **73**, 2634 (2002).
[37] B. Dick, Phys. Chem. Chem. Phys. **16**, 570 (2014).
[38] J. Cooper and R. N. Zare, J. Chem. Phys. **48**, 942 (1968).
[39] M. Vandevraye, C. Drag, and C. Blondel, Phys. Rev. A **85**, 015401 (2012).
[40] D. Bresteau, P. Babilotte, C. Drag, and C. Blondel, J. Phys. B: At., Mol. Opt. Phys. **48**, 125001 (2015).
[41] D. Bresteau, C. Drag, and C. Blondel, Phys. Rev. A **93**, 013414 (2016).
[42] E. P. Wigner, Phys. Rev. **73**, 1002 (1948).
[43] X. L. Chen and C. G. Ning, J. Chem. Phys. **145**, 084303 (2016).
[44] D. Bresteau, C. Drag, and C. Blondel, J. Phys. B: At., Mol. Opt. Phys. **52**, 065001 (2019).
[45] A. Osterwalder, M. J. Nee, J. Zhou, and D. M. Neumark, J. Chem. Phys. **121**, 6317 (2004).
[46] J. Neijzen and A. Dönszelmann, Physica B+C **114**, 241 (1982).
[47] T. Shirai, J. Reader, A. E. Kramida, and J. Sugar, J. Phys. Chem. Ref. Data **36**, 509 (2007).
[48] E. Tiesinga, P. J. Mohr, D. B. Newell, and B. N. Taylor, 2018 NIST CODATA recommended values of the fundamental physical constants, NIST, Gaithersburg, MD, http://physics.nist.gov/constants; retrieved 2019.
[49] Y. Liu and C. G. Ning, J. Chem. Phys. **143**, 144310 (2015).
[50] H. Bethe, *Quantentheorie* (Springer Berlin Heidelberg, Berlin, Heidelberg, 1933).
[51] C. W. Walter, J. A. Seifert, and J. R. Peterson, Phys. Rev. A **50**, 2257 (1994).
[52] R. C. Bilodeau and H. K. Haugen, Phys. Rev. Lett. **85**, 534 (2000).